

# RESEARCH MEMORANDUM

FULL-SCALE INVESTIGATION OF A WING WITH THE LEADING  
EDGE SWEPT BACK  $47.5^{\circ}$  AND HAVING CIRCULAR-ARC AND  
FINITE-TRAILING-EDGE-THICKNESS AILERONS

By

Roy H. Lange

Langley Aeronautical Laboratory  
Langley Air Force Base, Va.

NATIONAL ADVISORY COMMITTEE  
FOR AERONAUTICS  
WASHINGTON

March 11, 1949  
Declassified August 18, 1954

U  
NATIONAL ADVISORY COMMITTEE FOR AERONAUTICS

## RESEARCH MEMORANDUM

---

---

FULL-SCALE INVESTIGATION OF A WING WITH THE LEADING  
EDGE SWEPT BACK  $47.5^\circ$  AND HAVING CIRCULAR-ARC AND  
FINITE-TRAILING-EDGE-THICKNESS AIERONS

By Roy H. Lange

## SUMMARY

The results of an investigation in the Langley full-scale tunnel to determine the aerodynamic characteristics of a wing with the leading edge swept back  $47.5^\circ$  and having a 20-percent-chord, 50-percent-span outboard aileron are presented in this paper. The wing had symmetrical circular-arc airfoil sections and was investigated both with a circular-arc contour aileron and with a flat-sided contour aileron with finite trailing-edge thickness. Tests were also made to determine the aileron effectiveness with and without the modified aileron. All the data are presented for a Reynolds number of about  $4.3 \times 10^6$  and a Mach number of about 0.07.

The results show that the finite-trailing-edge-thickness aileron caused about a 3-percent stabilizing shift in the aerodynamic-center location as compared with the basic wing for a lift-coefficient range of 0 to 0.35. The finite-trailing-edge-thickness aileron caused about a 15-percent increase in drag coefficient for lift coefficients below 0.3. In general, the finite-trailing-edge-thickness aileron gave a more nearly linear variation of rolling-moment coefficient with aileron deflection for a range of angle of attack from  $0^\circ$  to  $16^\circ$  by eliminating the reduction in aileron effectiveness for deflections between  $10^\circ$  and  $15^\circ$  characteristic of the basic wing aileron. For angles of attack greater than  $16^\circ$  there is no appreciable difference in the effectiveness of the two aileron configurations.

## INTRODUCTION

The problem of securing adequate lateral control for high-speed aircraft employing sweptback wings requires careful consideration for both the high-speed and the low-speed flight conditions. An investigation at high subsonic and transonic speeds ( $M = 0.50$  to  $1.2$ ) of a 20-percent-chord, 50-percent-span outboard aileron on a  $42.7^\circ$  sweptback wing showed that changing the circular-arc aileron contour to a flat-sided aileron contour with finite trailing-edge thickness eliminated

reversal of control in most cases and generally improved the aileron control characteristics (reference 1). In addition, an investigation at a Mach number of 1.9 (reference 2) also showed some improvement in rolling effectiveness resulting from the use of the thick aileron. Inasmuch as the aileron with finite trailing-edge thickness produced desirable control characteristics for high-speed flight, it was of particular interest to determine the characteristics of this aileron for low-speed, high-altitude flight conditions. Therefore, incidental to a general investigation in the Langley full-scale tunnel of a 47.5° sweptback wing with symmetrical circular-arc airfoil sections, tests were made of the wing with a 20-percent-chord, 50-percent-span outboard aileron with both the circular-arc contour and the flat-sided contour with finite trailing-edge thickness. A trailing-edge thickness of one-half the aileron-hinge-line thickness was tested inasmuch as the results of reference 1 indicated that, in general, this configuration was more effective than other trailing-edge thicknesses.

The investigation included measurements at a Reynolds number of about  $4.3 \times 10^6$  and a Mach number of about 0.07 of the lift, the drag, and the pitching-moment coefficients of the basic wing and of the wing with the finite-trailing-edge-thickness aileron installed for a large angle-of-attack range. The aileron effectiveness was also determined for the two aileron configurations from tests with the right aileron deflected through a range from 0° to 19.6°.

#### COEFFICIENTS AND SYMBOLS

The test data are presented as standard NACA coefficients of forces and moments. The data are referred to a set of axes coinciding with the wind axes, and the origin was located at the quarter-chord point of the mean aerodynamic chord.

$C_L$	lift coefficient $\left( \frac{\text{Lift}}{qS} \right)$
$C_D$	drag coefficient $\left( \frac{\text{Drag}}{qS} \right)$
$C_m$	pitching-moment coefficient $\left( \frac{M}{qS\bar{c}} \right)$
$C_l$	rolling-moment coefficient $\left( \frac{L}{qSb} \right)$
$C_{l_a}$	rolling-moment coefficient produced by the aileron
$M$	pitching moment or free-stream Mach number
$L$	rolling moment

$\alpha$	angle of attack, degrees
$q$	free-stream dynamic pressure
$S$	wing area (231.0 sq ft)
$b$	wing span (28.5 ft)
$c$	mean aerodynamic chord measured parallel to plane of symmetry (8.37 ft) $\left( \frac{2}{S} \int_0^{b/2} c^2 dy \right)$
$\bar{x}$	distance from leading edge of root chord to quarter chord of the mean aerodynamic chord (9.03 ft) $\left( \frac{2}{S} \int_0^{b/2} cx dy \right)$
$t$	airfoil thickness
$\delta_{aR}$	right aileron deflection, positive for down deflections, degrees
$c$	chord, parallel to plane of symmetry
$x$	longitudinal distance, parallel to plane of symmetry, from leading edge of root chord to quarter-chord point of each section
$\frac{\partial C_m}{\partial C_L}$	rate of change of pitching-moment coefficient with lift coefficient
$\frac{\partial C_l_a}{\partial \delta_{aR}}$	rate of change of rolling-moment coefficient produced by aileron with right aileron deflection, per degree

## MODEL

The geometric characteristics of the wing are given in figure 1. The wing has an angle of sweepback of  $45^\circ$  at the quarter-chord line, an aspect ratio of 3.5, a taper ratio of 0.5 and has no geometric dihedral or twist. The airfoil section of the wing is a symmetrical, 10-percent-thick, circular-arc section perpendicular to the 50-percent-chord line. A more detailed description of the wing is given in reference 3.

The aileron tested was actually an outboard 50-percent-span, 20-percent-chord (normal to the 50-percent-chord line) trailing-edge plain flap. This flap was pivoted on piano hinges mounted flush with the lower

wing surface and, therefore, only downward deflections were possible. When the flap was deflected the gap on the upper wing surface was covered and faired with a sheet-metal seal. Aileron deflections of  $0^\circ$ ,  $5.7^\circ$ ,  $10.2^\circ$ ,  $14.3^\circ$ , and  $19.6^\circ$  were provided on the right aileron only. A sketch of the aileron contours tested is given in figure 2, and a photograph of the wing with the aileron modified with a finite trailing-edge thickness is given as figure 3.

### TESTS

All the tests were made through an angle-of-attack range from about  $-2^\circ$  to  $25^\circ$  and at a Reynolds number of about  $4.3 \times 10^6$  and a Mach number of about 0.07. In order to determine the longitudinal characteristics of the wing measurements were made of the lift, the drag, and the pitching-moment coefficients of the basic wing and of the wing with the modified aileron. The aileron-effectiveness tests were made with only the right aileron deflected through a range from  $0^\circ$  to  $19.6^\circ$ . For these tests the aileron was set at the required deflection, and then force tests were made as the angle of attack of the wing was increased from  $0^\circ$  to  $25^\circ$ .

The effects of the aileron with finite trailing-edge thickness on the stall progression of the wing were determined from visual observations of the action of wool tufts attached to the upper wing surface.

### RESULTS AND DISCUSSION

The results have been corrected for the stream alinement, the blocking effects, the tares caused by the wing supports, and the jet-boundary effects which were calculated on the basis of an unswept wing.

#### Longitudinal Aerodynamic Characteristics

The finite-trailing-edge-thickness aileron shows a slight increase in lift-curve slope and in maximum lift coefficient as compared with the basic wing. (See fig. 4(a).) The drag coefficient of the basic wing is increased by about 15 percent for lift coefficients below 0.3 by the addition of the finite-trailing-edge-thickness aileron. (See fig. 4(b).)

As shown by the variations of  $C_m$  with  $C_L$  in figure 4(c), the aileron with finite trailing-edge thickness caused about a 3-percent stabilizing shift in the aerodynamic-center location as compared with the basic wing for a lift-coefficient range from 0 to 0.35. For lift coefficients above about 0.5, however, there is no appreciable change in aerodynamic-center location as compared with the basic wing.

Observations of the stall progression over the wing with the finite-trailing-edge-thickness aileron installed showed a delay in the angles of attack at which spanwise flow was fully developed in the outer wing semispan as compared with the flow over the basic wing. As a result, the flow over the outer wing semispan was improved through the low and moderate angle-of-attack range which resulted in an increase in the lift over this portion of the wing and more stabilizing pitching characteristics. However, at the higher angles of attack there was no significant difference in the stall progressions.

### Aileron Effectiveness

The rolling-moment data presented in figure 5 were used to obtain the aileron-effectiveness results presented in figure 6, and the rolling-moment coefficients presented in figure 6 represent the coefficient at a given deflection minus the coefficient at zero deflection. In general, the finite-trailing-edge-thickness aileron gave a more nearly linear variation of rolling-moment coefficient with aileron deflection for a range of angle of attack from  $0^\circ$  to  $16^\circ$  by eliminating the reduction in

the aileron effectiveness  $\frac{\partial C_{l_a}}{\partial \delta_{aR}}$  for deflections between  $10^\circ$  and  $15^\circ$

characteristic of the basic wing aileron. For angles of attack greater than  $16^\circ$ , there is no appreciable difference in the effectiveness of the

two aileron configurations. The aileron effectiveness  $\frac{\partial C_{l_a}}{\partial \delta_{aR}}$  at the highest deflection tested ( $\delta_{aR} = 19.6^\circ$ ) decreased from values

of  $-0.00118$  and  $-0.00148$  for the basic-wing aileron and finite-trailing-edge-thickness aileron, respectively, at an angle of attack of  $0^\circ$  to  $-0.00039$  for both aileron configurations at an angle of attack of  $20^\circ$ . The effectiveness is further decreased to about zero for both aileron configurations at an angle of attack of  $22^\circ$ . For these higher attitude conditions, each aileron produces about the same maximum rolling-moment coefficient of about  $-0.012$ .

### SUMMARY OF RESULTS

The results of an investigation in the Langley full-scale tunnel of a wing with the leading edge swept back  $47.5^\circ$  and having a 20-percent-chord, 50-percent-span aileron with a circular-arc contour and with a flat-sided contour with finite trailing-edge thickness showed the following:

1. The finite-trailing-edge-thickness aileron caused a 3-percent stabilizing shift in the aerodynamic-center location as compared with the basic wing for a lift-coefficient range from 0 to 0.35. For lift

coefficients above 0.5 there is no appreciable change in the aerodynamic-center location as compared with the basic wing.

2. The finite-trailing-edge-thickness aileron caused about a 15-percent increase in drag for lift coefficients below 0.3 and slightly increased the lift-curve slope and maximum lift coefficient.

3. In general, the finite-trailing-edge-thickness aileron gave a more nearly linear variation of rolling-moment coefficient with aileron deflection for a range of angle of attack from  $0^\circ$  to  $16^\circ$  by eliminating the reduction in aileron effectiveness for deflections between  $10^\circ$  and  $15^\circ$  characteristic of the basic wing aileron. For angles of attack greater than  $16^\circ$ , there is no appreciable difference in the effectiveness of the two aileron configurations.

Langley Aeronautical Laboratory  
National Advisory Committee for Aeronautics  
Langley Air Force Base, Va.

#### REFERENCES

1. Turner, Thomas R., Lockwood, Vernard E., and Vogler, Raymond D.: Aerodynamic Characteristics at Subsonic and Transonic Speeds of a  $42.7^\circ$  Sweptback Wing Model Having An Aileron with Finite Trailing-Edge Thickness. NACA RM No. L8K02, 1948.
2. Sivells, James C., and Conner, D. William: Preliminary Investigation at a Mach Number of 1.9 and a Reynolds Number of 2,200,000 of Three Ailerons Applicable to the Bell XS-2 Airplane Design. NACA RM No. L8D02, 1948.
3. Proterra, Anthony J.: Aerodynamic Characteristics of a  $45^\circ$  Swept-Back Wing with Aspect Ratio of 3.5 and NACA 2S-50(05)-50(05) Airfoil Sections. NACA RM No. L7C11, 1947.

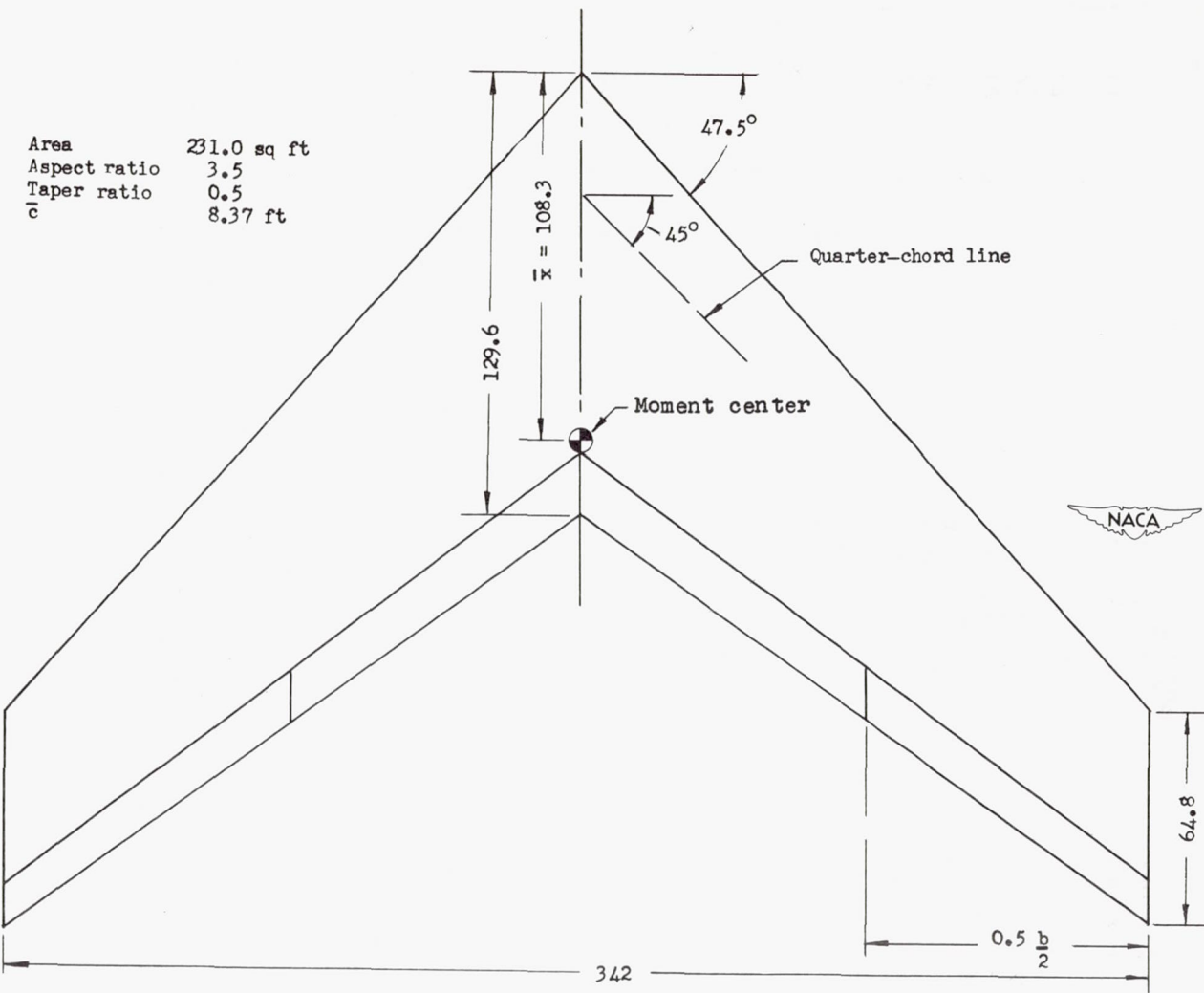
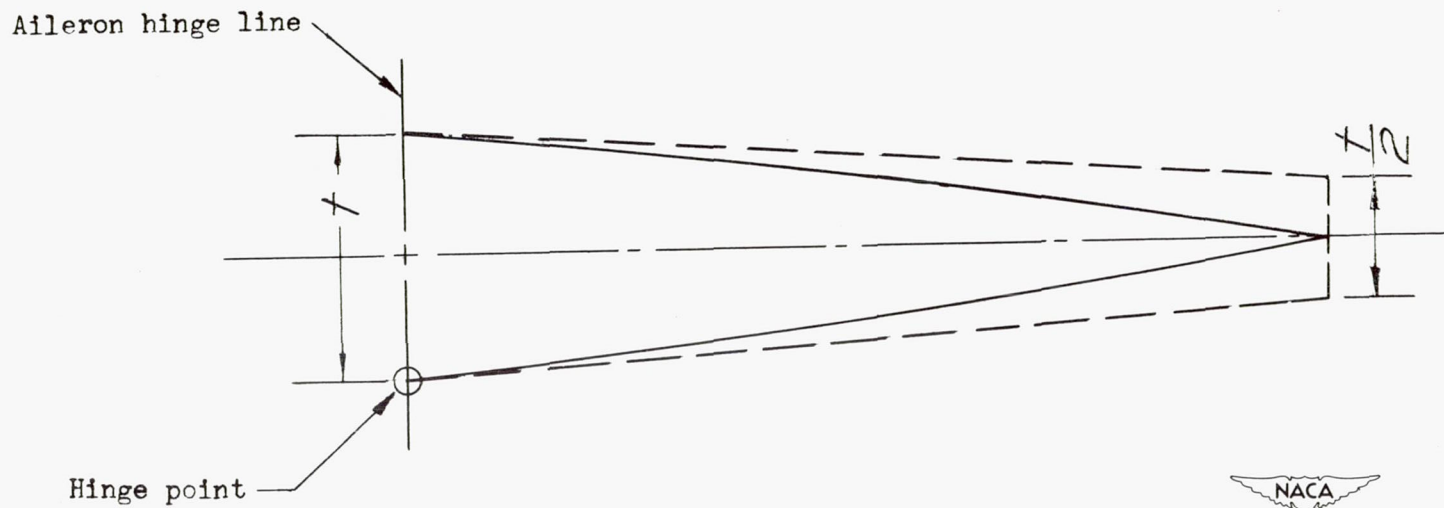


Figure 1.- Plan form of  $47.5^\circ$  sweptback wing. All dimensions are given in inches.

Spanwise location, $t/2$ , inches percent $b/2$	
50	2.33
75	1.97
100	1.61



— Basic aileron (circular arc)

— Finite-trailing-edge thickness aileron

Figure 2.- Section profiles of ailerons tested.

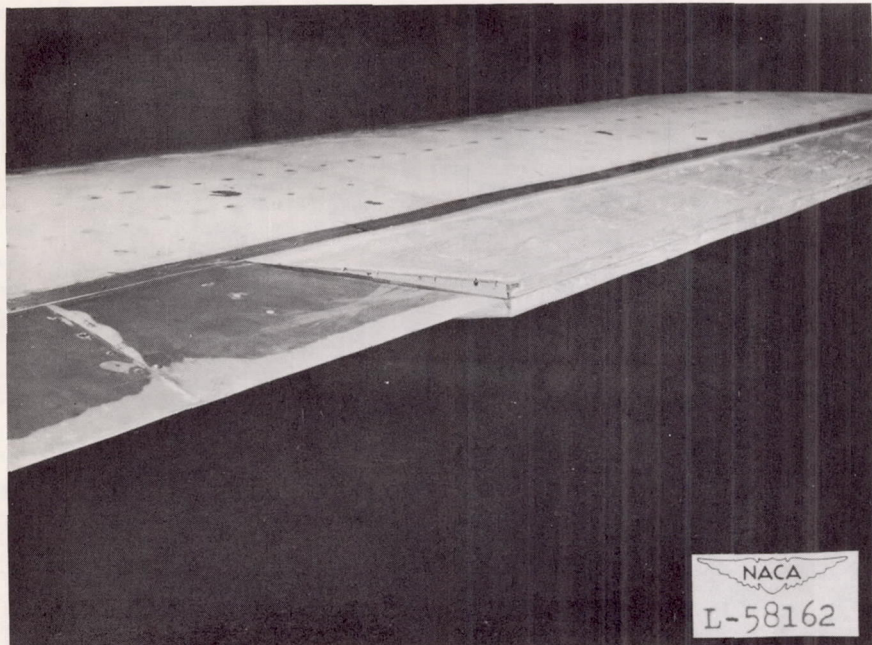
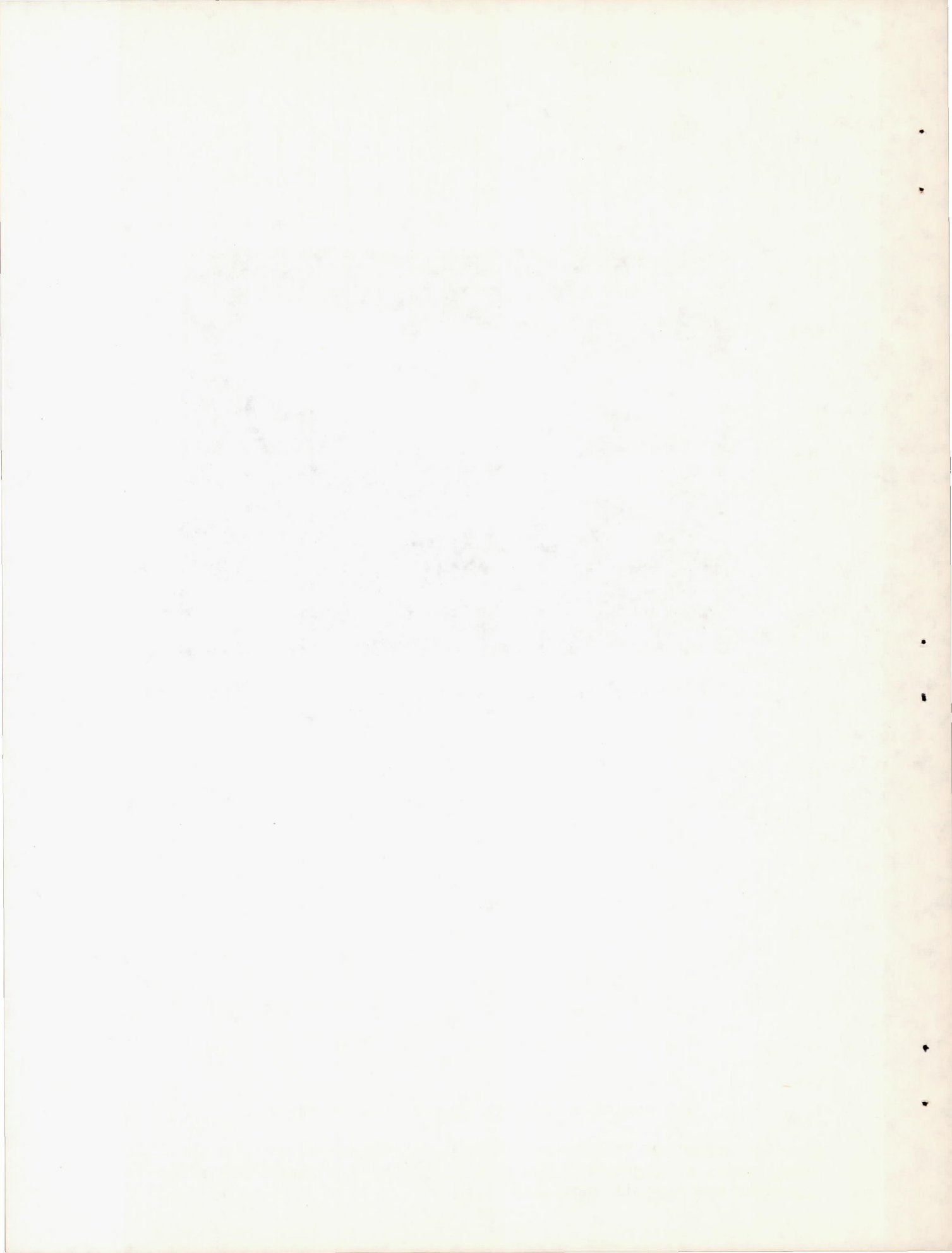


Figure 3.- Three-quarter rear view of wing with finite-trailing-edge-thickness aileron installed.



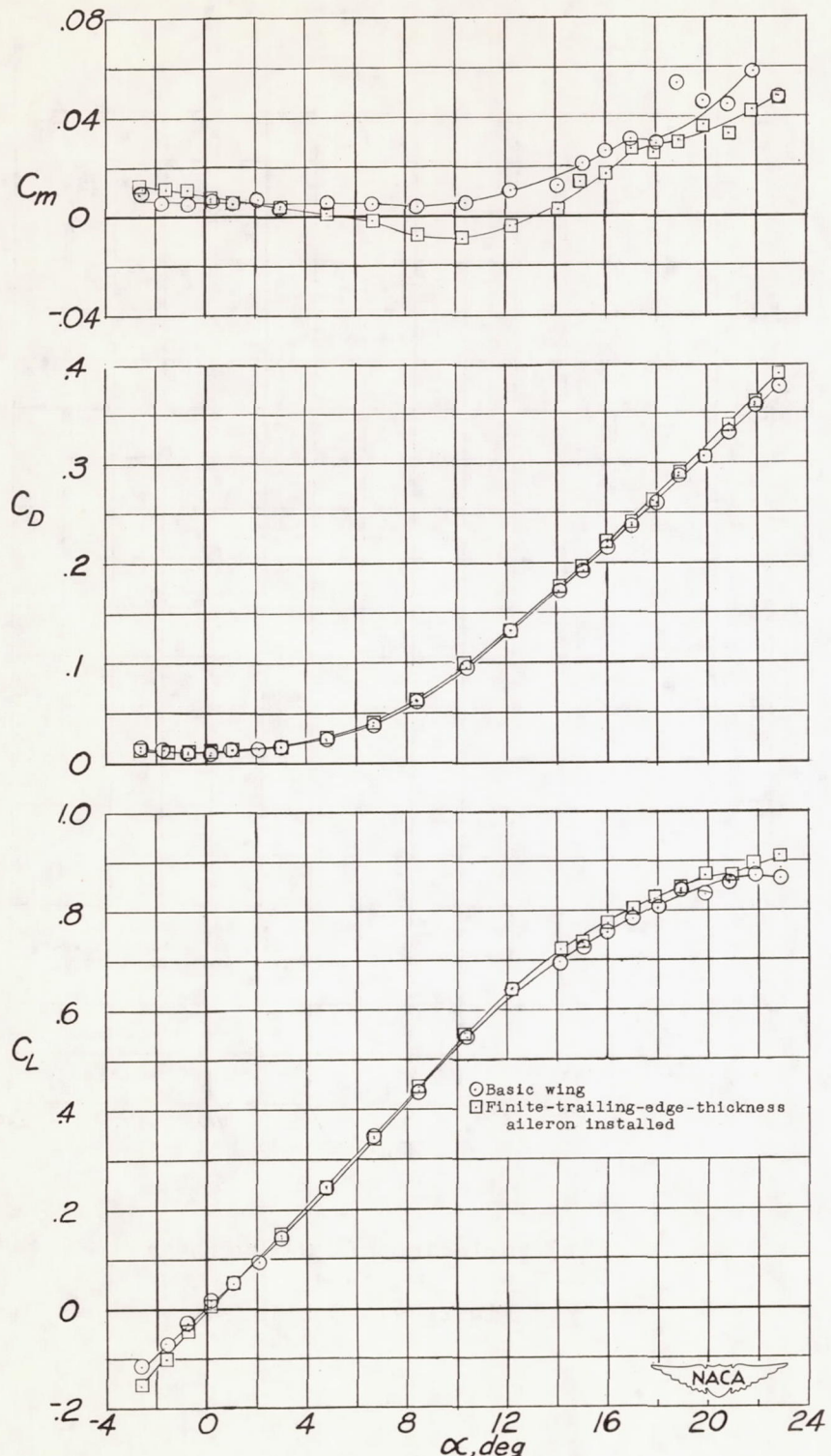
(a) Variation of  $C_L$ ,  $C_D$ , and  $C_m$  with  $\alpha$ .

Figure 4.- Effect of finite-trailing-edge-thickness aileron on the lift, drag, and pitching-moment coefficients of a  $47.5^\circ$  sweptback wing with circular-arc airfoil sections.  $\delta_{aR}$ ,  $0^\circ$ .

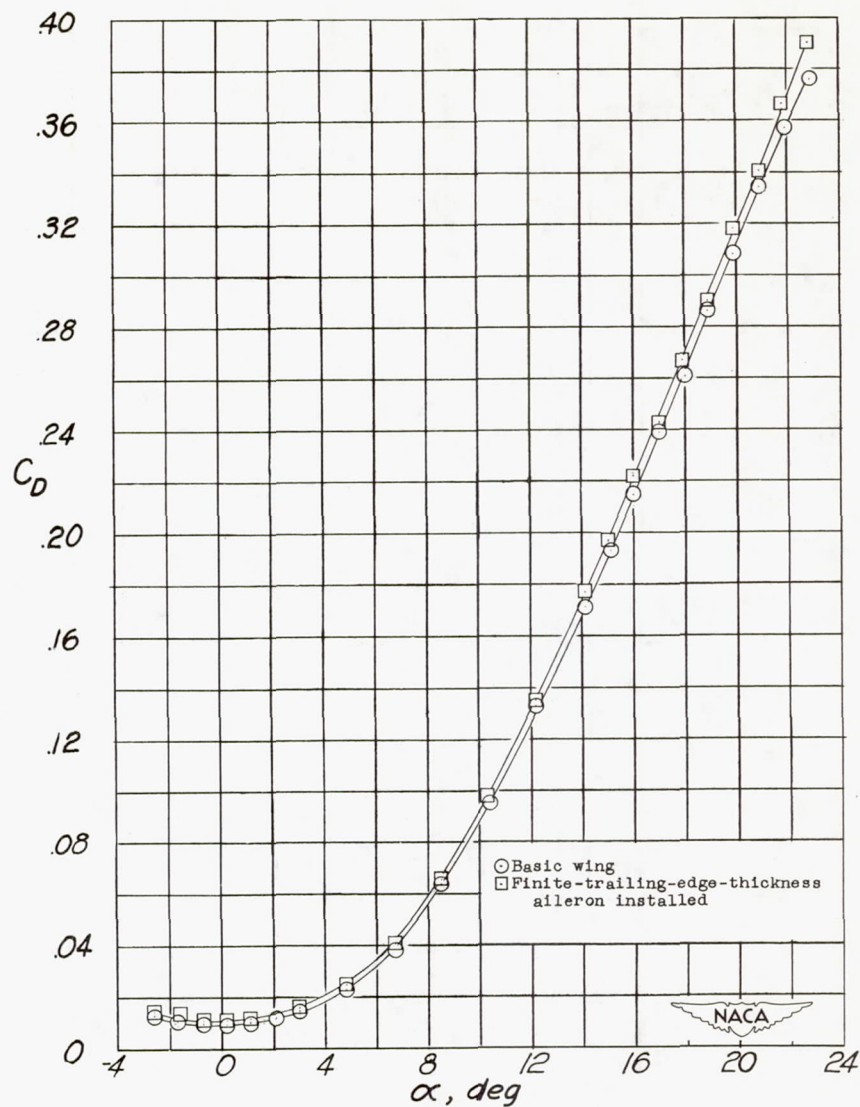
(b) Variation of  $C_D$  with  $\alpha$ .

Figure 4.- Continued.

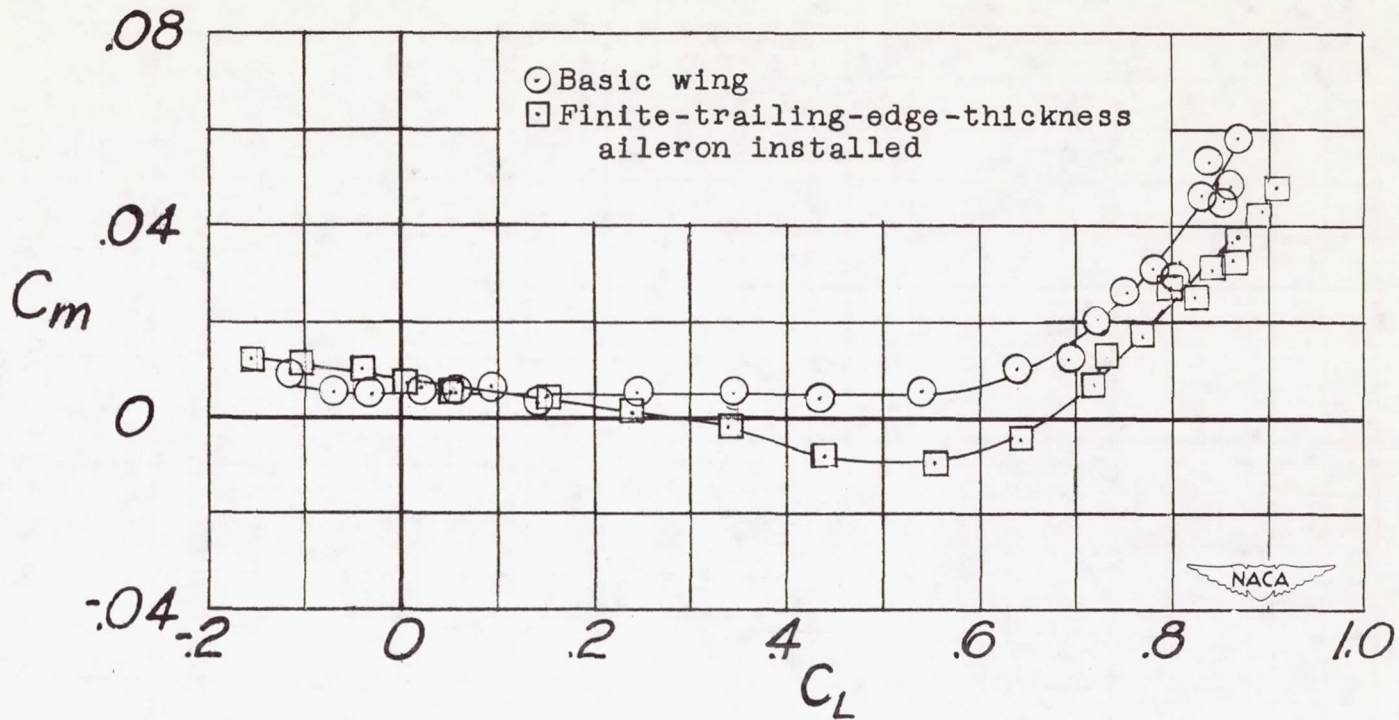
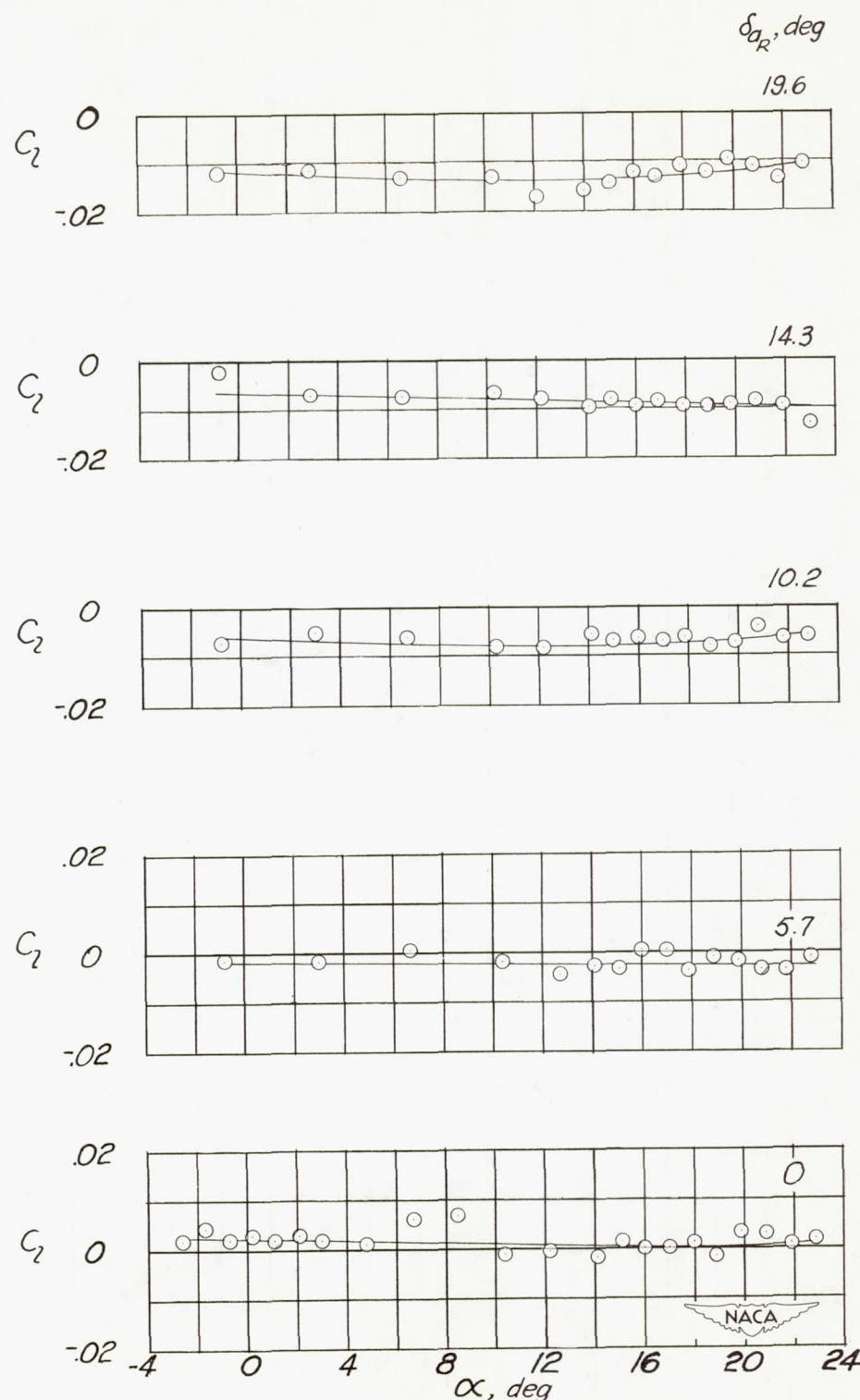
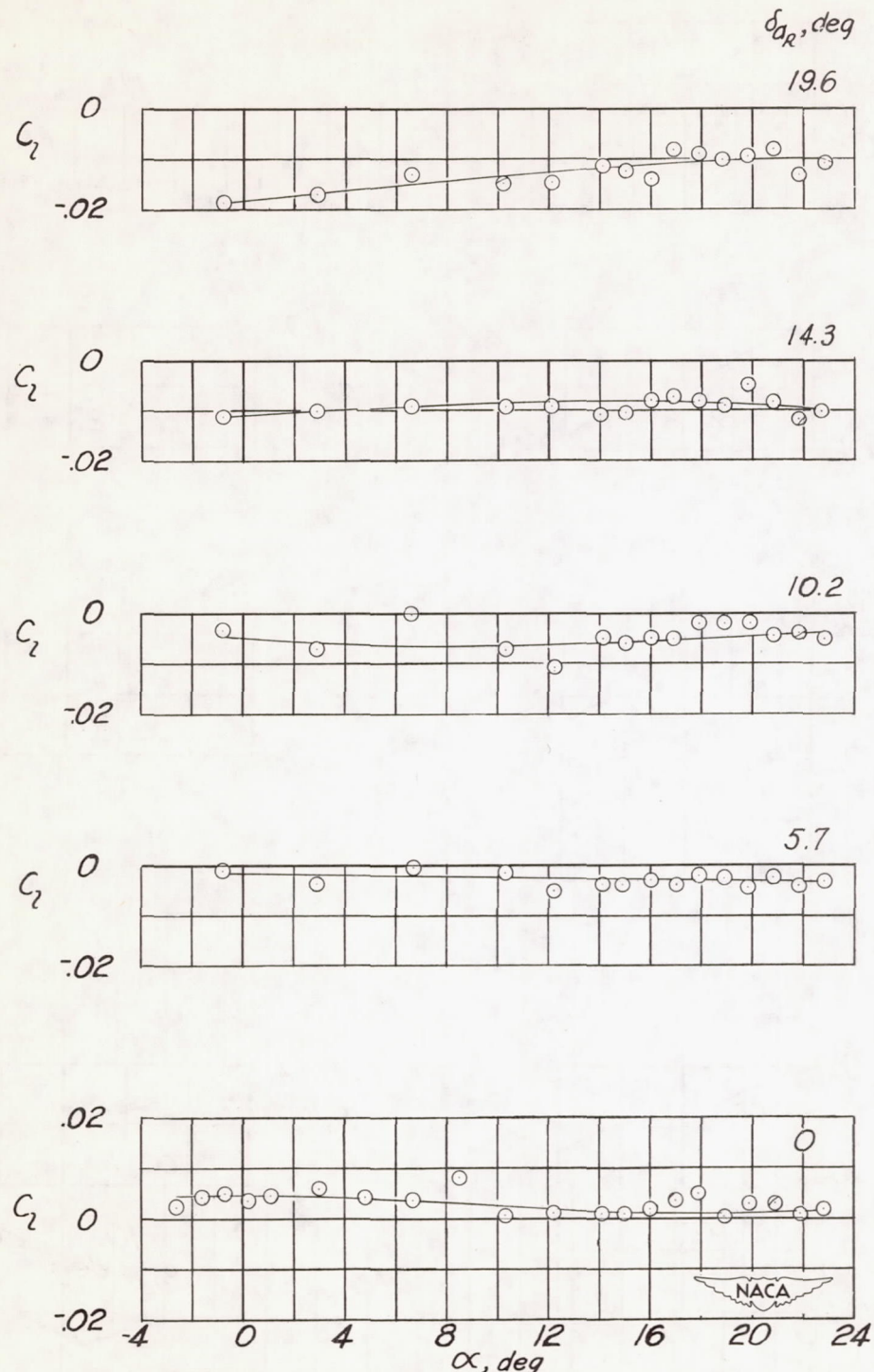
(c) Variation of  $C_m$  with  $C_L$ .

Figure 4.- Concluded.



(a) Basic wing aileron.

Figure 5.- Variation of rolling-moment coefficient with angle of attack for several aileron deflections.



(b) Finite-trailing-edge-thickness aileron installed.

Figure 5.- Concluded.

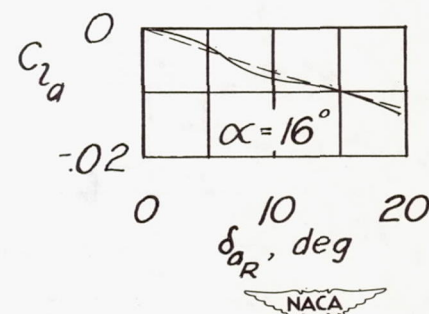
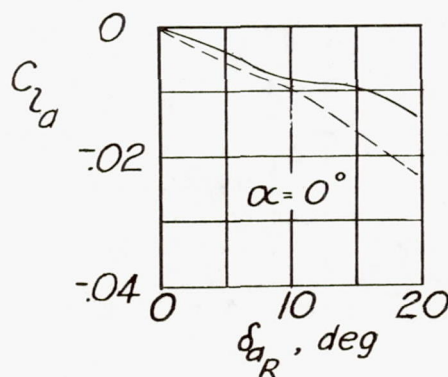
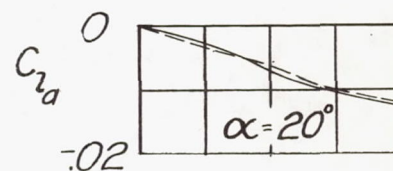
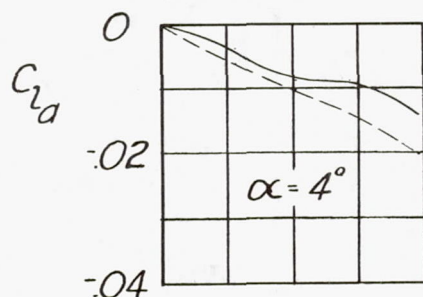
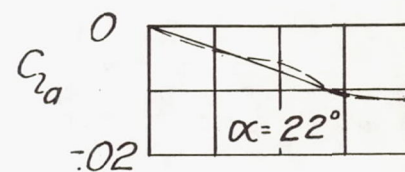
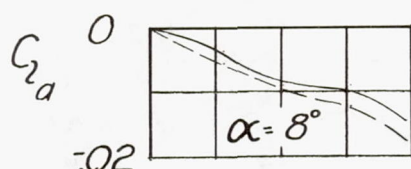
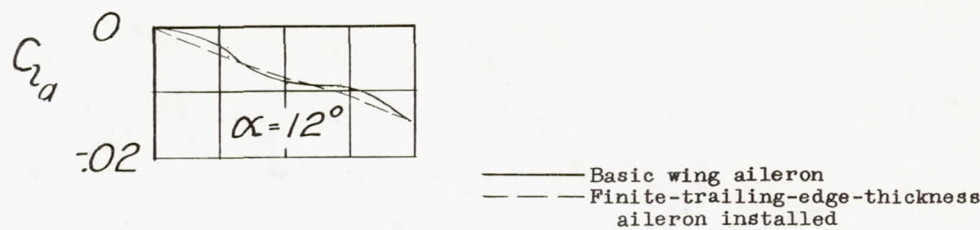


Figure 6.- Effect of finite-trailing-edge-thickness aileron on aileron effectiveness.